Precise Numerical Simulation of Microwave Scattering from Natural Deciduous Leaves Using the Method of Moment

Yisok Oh and Jin-Young Hong*
Department of Radio Science and Communication Engineering, Hongik University,
72-1 Sangsu-Dong, Mapo-Gu, Seoul, Korea. 121-791
yisokoh@hongik.ac.kr, nir26@hanmail.net

Abstract: A numerical algorithm using the Method of Moments (MoM) is introduced to compute precisely the scattering matrices of very thin deciduous leaves in this paper. At first, a dyadic Green's function was formulated and an integral equation for a volumetric current distribution in a lossy dielectric body. Then, the MoM was applied to the scattering problem with a specific technique to handle the numerical poles. The accuracy of the numerical technique was verified by examining the technique with various ways, and used to examine the validity regions of the classical analytical models.

Keywords: Method of Moment, thin deciduous leaf, microwave scattering.

1. Introduction

The classical scattering models such as the physical optics (PO) model, the Rayleigh model and the generalized Rayleigh-Gans (GRG) model, are commonly used to compute the radar cross sections (RCS) or the scattering matrices of deciduous leaves at microwave frequencies. The models have their own validity regions depending on the sizes of the leaves with respect to wavelengths of the electromagnetic waves [1-2]. The precise computation of the polarimetric scattering matrix of a deciduous leaf is required in order to judge the validity regions of the classical scattering models. Various numerical methods were reported to compute the scattering matrix of a lossy dielectric structure [3]. However, the numerical computation of the microwave scatter from a deciduous leaf is a challenging problem, because the leaf is very thin, especially at lower part of the microwave frequency band. In this paper, a numerical algorithm using the Method of Moments (MoM) is introduced to compute precisely the scattering matrices of very thin deciduous leaves, *i.e.*, thickness is less then $\lambda/100$, where λ is wavelength. At first, an integral equation was formulated with a dyadic Green's function [4], and then, the MoM was applied to compute accurate scattering matrices from the thin leaves. The computation results are compared with the classical scattering models, and the validity regions of the models are verified.

2. Formulation

For electromagnetic scattering from a lossy dielectric body, the following formulation for the equivalent volume current $\bar{J}(\bar{r}')$ has usually been used.

$$\bar{J}(\bar{r}') = -i\omega\varepsilon[\varepsilon_r - 1]\bar{E}(\bar{r}'), \tag{1}$$

where ε_r is the complex dielectric constant of the lossy dielectric body and $\bar{E}(\bar{r}')$ is the total electric field including the incident and scattered fields, $\bar{E} = \bar{E}^i + \bar{E}^s$.

A volume current density $\bar{J}(\bar{r})$ is induced in the dielectric body with an incident electric field of

$$\bar{E}^i(\bar{r}) = \hat{q}_i\, E_0\, e^{ik_0 \hat{k}_i \cdot \bar{r}}, \tag{2}$$

where $\hat{q}_i = \hat{v}_i$ or $\hat{h}_i$, $k_0 = 2\pi/\lambda_0$, and a time convention of $\exp[-i\omega t]$ is assumed. Then, the electric fields scattered from the dielectric body are computed using the electric current density $\bar{J}(\bar{r}')$ and the dyadic Green's function $\bar{\bar{G}}(\bar{r},\bar{r}')$ by

$$\bar{E}^s(\bar{r}) = ik_o\eta_0 \int_V \bar{\bar{G}}(\bar{r},\bar{r}')\cdot\bar{J}(\bar{r}')dv'. \tag{3}$$

where $\eta_0 = \sqrt{\mu_0/\varepsilon_0}$, and with

$$\bar{\bar{G}}(\bar{r},\bar{r}') = \left(\bar{\bar{I}} + \frac{\nabla\nabla}{k^2}\right)G(\bar{r},\bar{r}') \quad \text{and} \tag{4}$$

$$G(\bar{r},\bar{r}') = \frac{e^{ik|\bar{r}-\bar{r}'|}}{4\pi|\bar{r}-\bar{r}'|}. \tag{5}$$

Therefore, an integral equation can be obtained by substituting (2-3) into (1) as

$$\bar{J}(\bar{r}) - k_0^2(\varepsilon_r - 1)\int_V \bar{\bar{G}}(\bar{r},\bar{r}')\cdot\bar{J}(\bar{r}')\,dv' = -i\omega\varepsilon_0(\varepsilon_r - 1)\bar{E}^i(\bar{r}). \tag{6}$$

The unknown current density $\bar{J}(\bar{r})$ can be computed numerically using the method of moment (MoM). Among many other bases functions, the volumetric brick was chosen as the basis function in the limit of electrically small subdomains for simplicity. Using the point matching technique, the integral equation (6) can be cast into the following matrix equation,

$$\begin{bmatrix} [Z_{mn}^{xx}] & [Z_{mn}^{xy}] & [Z_{mn}^{xz}] \\ [Z_{mn}^{yx}] & [Z_{mn}^{yy}] & [Z_{mn}^{yz}] \\ [Z_{mn}^{zx}] & [Z_{mn}^{zy}] & [Z_{mn}^{zz}] \end{bmatrix} \begin{bmatrix} [I_n^x] \\ [I_n^y] \\ [I_n^z] \end{bmatrix} = \begin{bmatrix} [V_m^x] \\ [V_m^y] \\ [V_m^z] \end{bmatrix}, \tag{7}$$

where I_n^p is an unknown constant of the nth basis function for the p-component of the volume currents (p=x, y, z), and

$$V_m^p = -i\omega\varepsilon_0[\varepsilon_r(\bar{r}_m) - 1]\hat{q}\, e^{ik_0\hat{k}_i\cdot\bar{r}_m}\cdot\hat{p} \tag{8}$$

$$Z_{mn}^{pq} = \delta_{pq}\delta_{mn} - k_0^2[\varepsilon_r(\bar{r}_m)-1] \cdot \int_{\Delta V_n} G_{pq}(\bar{r}_m,\bar{r}_n)dv_n, \quad p,q = x,y,z \cdot \quad (9)$$

where δ_{pq} and δ_{mn} are the Kronecker delta functions, and $\bar{r}_m$ and $\bar{r}_n$ represent the mth matching position (observation point) and the nth integration position, respectively. The elements of the dyadic Green's function are found to be

$$G_{pp}(\bar{r}_m,\bar{r}_n) = G(R) + \frac{1}{k_0^2}\frac{\partial^2 G(R)}{\partial p^2}, \quad (10a)$$

$$G_{pq}(\bar{r}_m,\bar{r}_n) = \frac{1}{k_0^2}\frac{\partial^2 G(R)}{\partial p \partial q}, \quad p \neq q, \quad (10b)$$

where $p,q = x,y,z$ and $R = |\bar{r}_m - \bar{r}_n|$. Explicit form of differentiations of the Green's functions in (10) are given by

$$\frac{\partial^2 G(R)}{\partial p^2} = G(R)\left\{\frac{p_{mn}^2 f_1}{R^4} - \frac{(1-ik_0R)}{R^2}\right\}, \quad (11a)$$

$$\frac{\partial^2 G(R)}{\partial p \partial q} = G(R)\frac{p_{mn}q_{mn}f_1}{R^4}, \quad p \neq q, \quad (11c)$$

where $p,q = x,y,z$, $p_{mn} \equiv p_m - p_n$, $q_{mn} \equiv q_m - q_n$, and $f_1 = 3 - i3k_0R - k_0^2R^2$.

When n=m, the second derivatives of the Green's function $G(R)$ produces the well-known singularity. However, we can avoid this singularity by introducing an auxiliary function $g \equiv 1/4\pi R$ and subdividing the integral region to a small sphere V_ε centered at the observation point and the other part:

$$\int_{\Delta V_n} G_{pp}\,dv = \int_{\Delta V_n - V_\varepsilon} G_{pp}\,dv + \int_{V_\varepsilon} G\,dv + \frac{1}{k_0^2}\left[\int_{V_\varepsilon}\frac{\partial^2}{\partial p^2}(G-g)dv + \int_{V_\varepsilon}\frac{\partial^2}{\partial p^2}g\,dv\right]. \quad (12)$$

We can evaluate the integrals in the parenthesis in (12) explicitly for a small sphere with radius a, which leads to $-(1-ika)e^{ika}/3$. The integral of the second term in (12) can also be explicitly evaluated, and leads to $\{-1+(1-ika)e^{ika}\}/k_0^2$. Therefore, (12) becomes

$$\int_{\Delta V_n} G_{pp}\,dv_n = \int_{\Delta V_n - V_\varepsilon} G_{pp}\,dv_n + \frac{1}{k_0^2}\left\{-1+\frac{2}{3}(1-ika)e^{ika}\right\} \quad (13)$$

where p=x, y, z. The first integral of the right side of (13) was evaluated using a numerical integration technique.

Once the elements of the impedance matrix $[Z]$ and the excitation vector $[V]$ were calculated, the unknown equivalent volume current $[I]$ inside the dielectric body can be found by inverting (7). Consequently, the scattering field $\bar{E}^s(\bar{r})$ can be computed using (3). In the far zone, the scattered fields can be calculated with the following approximated equations:

$$\bar{\bar{G}}(\bar{r},\bar{r}') \approx (\hat{v}_s\hat{v}_s + \hat{h}_s\hat{h}_s)G(\bar{r},\bar{r}') \text{ and } \quad (14)$$

$$G(\bar{r},\bar{r}') \approx \frac{e^{ikr}}{4\pi r}e^{-ik\hat{k}_s\cdot\bar{r}'}.$$

The scattered field vector is related to the incident field vector in terms of a dyadic scattering amplitude $\bar{\bar{S}}$ as follows:

$$\bar{E}^s(\bar{r}) = \frac{e^{ikr}}{r}\bar{\bar{S}}(\hat{k}_s,\hat{k}_i)\cdot\hat{q}_iE_0 \quad (15)$$

where the scattering amplitude S_{pq} for a q-polarized incident wave and a p-polarized scattered wave can be written by

$$S_{pq} \equiv \hat{p}_s\cdot\bar{\bar{S}}(\hat{k}_s,\hat{k}_i)\cdot\hat{q}_i. \quad (16)$$

Then, the RCS of the dielectric disk is computed by

$$\sigma_{pq} = 4\pi|S_{pq}|^2, \quad p,q = v,h. \quad (17)$$

3. Verification

A deciduous leaf can be assumed to be a dielectric circular or elliptical disk with a thickness t of about 0.04 *cm*. The thickness is very small comparing with wavelength; *e.g.*, about $\lambda/140$ for 5.3 GHz. If we use cubic cells for the MoM, the size of matrix for the problem will be very large: *e.g.*, 19600 x 19600 for a 1 λ x 1 λ dielectric disk. Therefore, we need to use thin-disk-type cells for the MoM computation with precise manipulation. In this section, the computation process will be introduced with verification of the preciseness.

The dielectric constants of the leaf, corresponding to the gravimetric moisture content of Vg (g/cm^3), are obtained from an empirical formula for a given frequency. For an example, Vg=0.6 g/cm^3 corresponds ε_r=(19.2, 6.4) at 5.3 GHz.

Fig. 1 (a) shows a side view of a dielectric disk. The Generalized Rayleigh-Gans (GRG) model uses a dielectric spheroid for a deciduous leaf, while the physical optics (PO)/ Resistive sheet Model uses a current sheet as shown in Fig. 1 (a). In this figure, the thickness t and diameter D are $\lambda/140$ and 1 λ, respectively, as an example. The leaf can be any shape for the computation, and Fig. 1 (b) shows a circular disk as an example, which was divided by 305 $\lambda/20 \times \lambda/20 \times \lambda/140$ cells.

The first step of the verification is to compare the computation results of a simple structure with other computation outputs reported in literature. Fig. 2 shows excellent agreement between the bistatic scattering radar cross sections computed by this method and those reported in [5], for a dielectric cube with length of $a = \lambda/5$ and a dielectric constant of $\varepsilon_r = 9$.

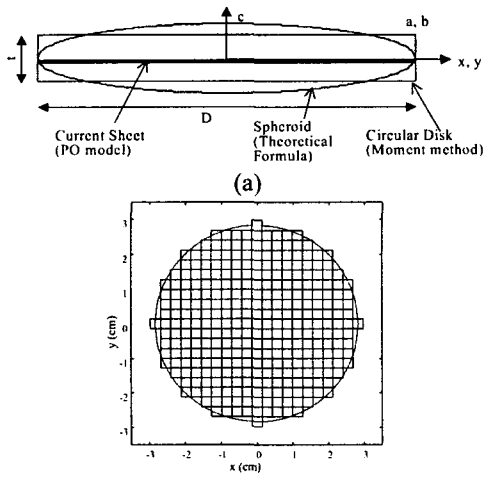

Fig. 1. Dielectric structure; (a) side view and (b) top view.

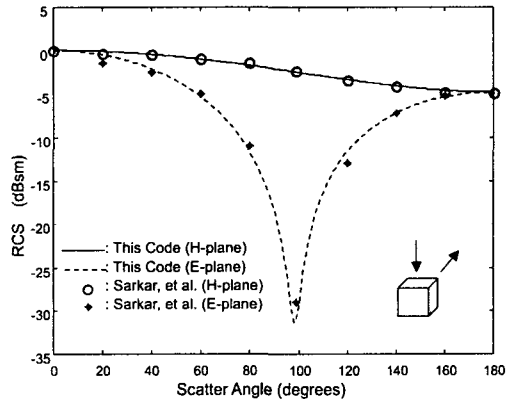

Fig. 2. Comparison of computation results for a dielectric cube ($a = \lambda/5$, $\varepsilon_r = 9$).

The second step of the verification is to examine the effect of the cell shape. The numerical integration for the diagonal terms of the impedance matrix elements was optimized with subdivision technique for thin cells. At first, the forward scatter RCS of a circular disk (D=1 λ and $t = \lambda/20$) divided with cubic cells ($\lambda/20 \times \lambda/20 \times \lambda/20$) was compared to the RCS with non-cubic cells ($\lambda/20 \times \lambda/20 \times \lambda/40$) at VV- and HH-polarizations as shown in Fig. 3 (a). For the latter case, the disk consists of two layers of $\lambda/40$ -thickness disks. It was shown that the code is good for non-cubic cell division. As the second test, backscatter RCS of a very thin lossy dielectric disk (D=1 λ and $t = \lambda/50$) was computed with two different types of cells. The disk was divided with $\lambda/20 \times \lambda/20 \times \lambda/50$ cells (cell 3) at the first case, and the disk was divided two layers and each layer consists with very thin $\lambda/20 \times \lambda/20 \times \lambda/100$ cells (cell 4). Fig. 3 (b) shows excellent agreement between the computation results with two different cell sizes.

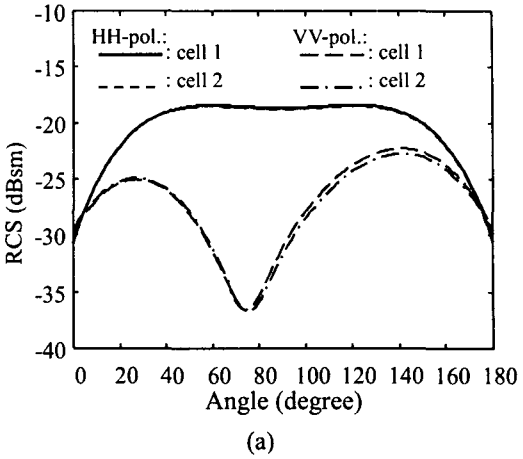

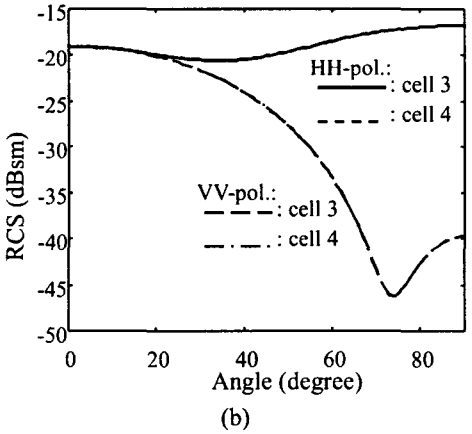

Fig. 3. Comparison of (a) the forward scattering RCS with $\theta_i = 60^o$ and (b) the backward scattering RCS for different cell types; *i.e.*, cell 1: $\lambda/20 \times \lambda/20 \times \lambda/20$, cell 2: $\lambda/20 \times \lambda/20 \times \lambda/40$, cell 3: $\lambda/20 \times \lambda/20 \times \lambda/50$, cell 4: $\lambda/20 \times \lambda/20 \times \lambda/100$,

4. Examination of Classical Models

The backscatter and forward-scatter RCSs are computed for a typical deciduous leaf. The leaf is an elliptical disk with a major axis of a=8cm, minor axis of b=3.5cm, a thickness t=0.04cm. The gravimetric moisture content of Vg (g/cm^3) corresponds ε_r =(19.2, 6.4) at 5.3 GHz.

The backscattering cross sections of the leaf were computed using the GRG and the PO approximations as well as the MoM at 5.3GHz for VV-polarizations over the range ($0^0 \le \theta \le 90^0$) as shown in Fig. 4. In this computation, the cell size of the elliptical dielectric disk for the MoM was 0.3cm x 0.3cm x 0.04cm ($\lambda/19$ x $\lambda/19$ x $\lambda/142$) and the number of the cell was 975 in this case. Both the GRG and PO models agree quite well with the MoM computation results except at large incidence angles ($\theta \ge 70^0$).

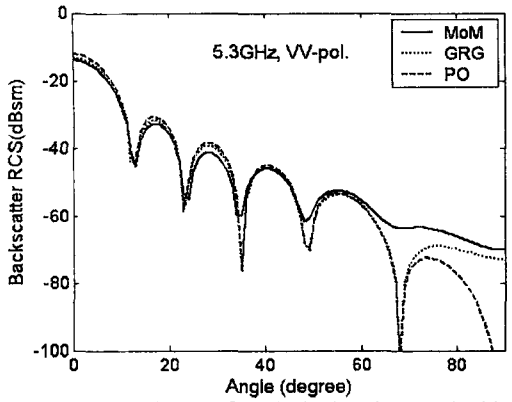

Fig.4. Comparisons of analytical and numerical backscatter RCSs of a leaf at 5.3GHz, VV-polarization

Fig. 5 shows the forward-scattering cross sections of the leaf, which are computed using the analytical and numerical models for VV-and HH-polarizations. The incidence wave has $\phi_s=0^0$, $0^0 \le \theta_s \le 180^0$. These figures also show that both analytical models agree quite well with the numerical solutions.

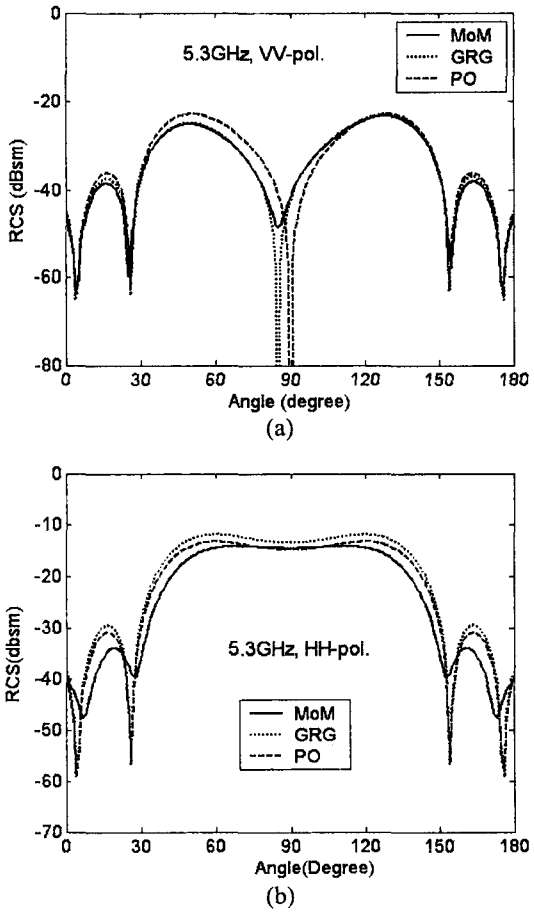

Fig.5. Comparisons of analytical and numerical forward-scatter RCSs of a leaf at 5.3GHz; (a) VV- and (b) HH-polarization

5. Concluding Remarks

A numerical algorithm using the MoM was introduced to compute precisely the scattering matrices of very thin deciduous leaves. At first, an integral equation for a volumetric current distribution in a lossy dielectric body was formulated. Then, the MoM was applied to the scattering problem with a specific technique to get precise scattering matrices for thin leaves. The accuracy of the numerical technique was verified by examining the technique with various ways, and used to examine the validity regions of the classical analytical models.

This numerical model can be used to predict precise radar scattering characteristics for various arbitrary-shaped scattering particles, such as coniferous leaves, vegetation leaves, branches, etc.

Acknowledgement

This work was supported from the Basic Technology Research Support Program of the Ministry of Information and Communication (Institute of Information Technology Assessment).

References

[1] F. T. Ulaby, K. Sarabandi, K. McDonald, M. Whitt and M. C. Dobson, "Michigan microwave canopy scattering model," *Int. J. Remote Sensing*, vol. 11, no. 7, pp. 1223-1253, 1990.

[2] M. A. Karam, A. K. Fung, R. H. Lang, and N. S. Chauhan, "A microwave scattering model for layered vegetation," *IEEE Trans. Geosci. Remote Sensing*, vol. 30, no. 4 pp. 767-784, July 1992.

[3] Y. Oh, Y-M. Jang and K. Sarabandi, "Full-wave analysis of microwave scattering from short vegetation: An investigation on the effect of multiple scattering," *IEEE Trans. Geosci. Remote Sensing*, vol. 40, no. 11, pp. 2522-2526, Nov. 2002.

[4] C. T. Tai, ***Generalized Vector and Dyadic Analysis: Applied Mathematics in Field Theory***, 2/e, IEEE Press, 1997.

[5] T. K. Sarkar, E. Arvas, and S. Ponnapalli, "Electromagnetic scattering from dielectric bodies," *IEEE Trans. Antennas Propagat.*, vol. AP-37, pp. 673-676, 1989.